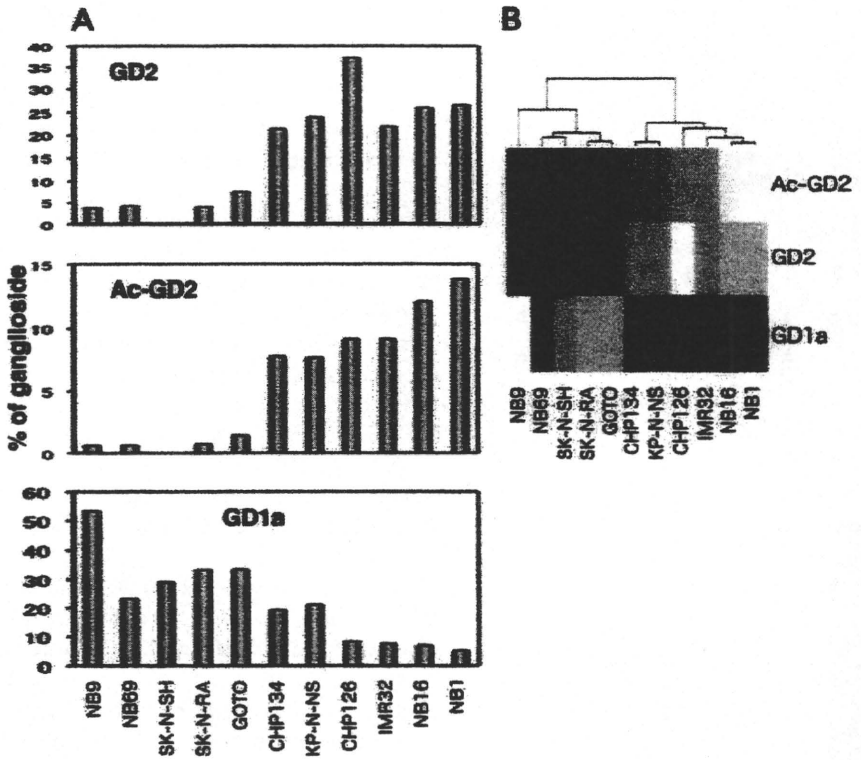

Figure 5. Hierarchical clustering of differentially expressed gangliosides. (A) The percentage of Ac-GD2, GD2 and GD1a to the total gangliosides of NB cell lines. (B) The clustering tree shows the expression pattern and similarity in cell lines. The strength of the gangioside expression was gradually increased on the heat map.

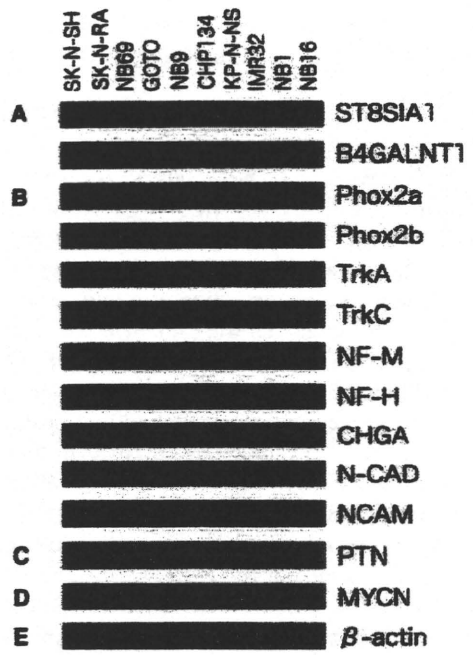

Figure 6. Analysis of expression of neural-differentiation-related genes and glycosyltransferase genes by RT-PCR. (A) Glycosyltransferase genes (Fig. 1). (B) *Phox2a*, paired-like (aristaless) homeobox 2a; *Phox2b*, paired-like homeobox 2b; *TrkA*, neurotrophic tyrosine kinase, receptor, type 1, also known as *NTRK1*; *TrkC*, neurotrophic tyrosine kinase, receptor, type 3, also known as *NTRK3*; *NF-M*, neurofilament 160 kDa subunit; *NF-H*, neurofilament 200 kDa subunit; *CHGA*, chromogranin A; *N-CAD*, N-cadherin and *NCAM*, neural cell adhesion molecule, (C) *PTN*, pleiotrophin, (D) *MYCN*, v-myc myelocytomatosis viral related oncogene, (E) ß-actin was used as an internal control.

The biological significance of ganglioside acetylation has not been fully elucidated, but it is thought to modulate cell function by regulating the ability of gangliosides to bind cell adhesion molecules. For example, CD22ß (also called Siglec-2) is a B-cell-restricted phosphoprotein that mediates interactions with other cells via binding with α2-6-linked sialic acids on glycoconjugates, and the fact that the binding can be inhibited by 9-O-acetylation of sialic acids suggests that CD22ß adhesion events are regulated by ganglioside acetylation (14,15). In childhood acute lymphoblastic leukemia, on the other hand, administration of exogenous GD3 induces apoptosis, whereas O-acetylated GD3 fails to induce similar effects, suggesting that O-acetylation of GD3 promotes leukemia cell survival by preventing apoptosis (16,17). Although the significance of acetylated GD2 in NB cells still remains largely unknown, further investigation should shed light on the functional role of gangliosides in the biological behavior of NB cells.

The NB cell lines were classified into three types based on their of ganglioside expression profiles determined by LC-MS analysis, namely, type A, with a high level of expression of GD1a but low level or no expression of GD2/acetylated GD2, and consisting of SK-N-SH, SK-N-RA, NB69, GOTO and NB9 cells, type B, with a high level of expression of GD2/acetylated GD2 but low level or no expression of GD1a, and consisting of IMR32, NB1, NB16 and CHP126 cells, and type AB, which express both GD1a and GD2/acetylated GD2, and consisting of CHP134 and KP-N-NS cells. The results of the RT-PCR analyses indicated that the ganglioside expression profiles of NBs correlated with their ganglioside

synthase expression pattern. As shown in Fig. 6, ST8sia1, which catalyzes the synthesis of GD3 from GM3, was expressed only in the types B and AB NB cell lines and not in any of the type A NB cell lines, whereas B4galnt1, which catalyzes the synthesis of both GM2 and GD2, was expressed in all the NB cell lines tested in this study.

Expression of GD2 ganglioside is characteristic of cells of neuroectodermal origin, and a high level of expression has been reported in NB cells, whereas the GD2 distribution in humans is limited to neurons and peripheral nerve fibers (18). Thus, GD2 appears to be useful as a target for the treatment of NB. However, our findings in this study indicated that the level of GD2 expression in NB cells is variable and that NB cells can be classified based on their pattern of expression of ganglio-series gangliosides, including GD2. Since increased shedding of GD2 ganglioside and *MYCN* amplification jointly characterize the aggressive type of NB cells (19), classification of NBs based on their ganglioside expression profile may have prognostic value. Our observation that the ganglioside expression profiles are closely related to the expression of neural-differentiation-related genes appears to further support this notion.

In conclusion, we have demonstrated the usefulness of the LC-MS analysis system as a tool for glycosphingolipid research. Eighteen species of glycosphingolipids containing gangliosides of a and b pathways and their acetylated forms were detected. The expression ratios of the glycosphingolipids were determined, and were compared among 11 of NB cell lines. Based on the results, it was indicated that these NB cell lines could be classified into three categories. Although more detailed experiments are clearly needed, further investigations using the new method should provide a new approach to determining the biological significance of glycosphingolipids in NBs and identifying novel biomarkers for predicting the outcome of NB.

Acknowledgments

We are grateful to Dr P. Reynolds for providing the SK-N-SH and SK-N-RA cells. We thank Ms. H. Kiyokawa for her assistance to prepare the manuscript. This work was supported by a grant from the Japan Health Sciences Foundation for Research on Publicly Essential Drugs and Medical Devices (KHA1004), Health and Labour Sciences Research Grants (Research on Human Genome Tailor made and Research on Publicly Essential Drugs and Medical Devices H18-005, the 3rd-term Comprehensive 10-year strategy for Cancer Control H19-010), a Grant for Child Health and Development from the Ministry of Health, Labour and Welfare of Japan, and by CREST, JST. This work was supported in part by the Grant-in-Aid for Cancer Research (16-16) from the Ministry of Health, Labor and Welfare.

References

1. Ledeen RW and Yu RK: Gangliosides: structure, isolation, and analysis. Methods Enzymol 83: 139-191, 1982.
2. Van Echten G and Sandhoff K: Ganglioside metabolism. Enzymology, topology, and regulation. J Biol Chem 268: 5341-5344, 1993.
3. Hakomori S: Tumor malignancy defined by aberrant glycosylation and sphingo(glyco)lipid metabolism. Cancer Res 56: 5309-5318, 1996.
4. Weinstein JL, Katzenstein HM and Cohn SL: Advances in the diagnosis and treatment of neuroblastoma. Oncologist 8: 278-292, 2003.
5. Ohira M, Oba S, Nakamura Y, Hirata T, Ishii S and Nakagawara A: A review of DNA microarray analysis of human neuroblastomas. Cancer Lett 228: 5-11, 2005.
6. Schengrund CL, Repman MA and Shochat SJ: Ganglioside composition of human neuroblastomas. Correlation with prognosis. A Pediatric Oncology Group Study. Cancer 56: 2640-2646, 1985.
7. Schengrund CL and Shochat SJ: Gangliosides in neuroblastomas. Neurochem Pathol 8: 189-202, 1988.
8. Kaucic K, Etue N, LaFleur B, Woods W and Ladisch S: Neuroblastomas of infancy exhibit a characteristic ganglioside pattern. Cancer 91: 785-793, 2001.
9. Hettmer S, Malott C, Woods W, Ladisch S and Kaucic K: Biological stratification of human neuroblastoma by complex B pathway ganglioside expression. Cancer Res 63: 7270-7276, 2003.
10. Wu ZL, Schwartz E, Seeger R and Ladisch S: Expression of GD2 ganglioside by untreated primary human neuroblastomas. Cancer Res 46: 440-443, 1986.
11. Nakamura K, Suzuki M, Taya C, Inagaki F, Yamakawa T and Suzuki A: A sialidase-susceptible ganglioside, IV3 alpha (NeuGc alpha 2-8NeuGc)-Gg4Cer, is a major disialoganglioside in WHT/Ht mouse thymoma and thymocytes. J Biochem 110: 832-841, 1991.
12. Kushi Y, Ogura K, Rokukawa C and Handa S: Blood group A-active glycosphingolipids analysis by the combination of TLC-immunostaining assay and TLC/SIMS mass spectrometry. J Biochem 107: 685-688, 1990.
13. Ye JN and Cheung NK: A novel O-acetylated ganglioside detected by anti-GD2 monoclonal antibodies. Int J Cancer 50: 197-201, 1992.
14. Sjoberg ER, Powell LD, Klein A and Varki A: Natural ligands of the B cell adhesion molecule CD22 beta can be masked by 9-O-acetylation of sialic acids. J Cell Biol 126: 549-562, 1994.
15. Kelm S, Schauer R, Manuguerra JC, Gross HJ and Crocker PR: Modifications of cell surface sialic acids modulate cell adhesion mediated by sialoadhesin and CD22. Glycoconj J 11: 576-585, 1994.
16. Malisan F, Franchi L, Tomassini B, *et al*: Acetylation suppresses the proapoptotic activity of GD3 ganglioside. J Exp Med 196: 1535-1541, 2002.
17. Mukherjee K, Chava AK, Mandal C, Dey SN, Kniep B, Chandra S and Mandal C: O-acetylation of GD3 prevents its apoptotic effect and promotes survival of lymphoblasts in childhood acute lymphoblastic leukaemia. J Cell Biochem 105: 724-734, 2008.
18. Varki A: Glycosylation changes in cancer. In: Essentials of Glycobiology. Varki A and Cummings R (eds). Cold Spring Harbor Laboratory Press, New York, 1999.
19. Valentino L, Moss T, Olson E, Wang HJ, Elashoff R and Ladisch S: Shed tumor gangliosides and progression of human neuroblastoma. Blood 75: 1564-1567, 1990.
20. Sekiguchi M, Oota T, Sakakibara K, Inui N and Fujii G: Establishment and characterization of a human neuroblastoma cell line in tissue culture. Jpn J Exp Med 49: 67-83, 1979.
21. Miyake S, Shimo T, Kitamura Y, Nojyo T, Nakamura S, Imashuku S and Abe T: Characteristics of continuous and functional cell line NB-1, derived from a human neuroblastoma. Autonomic Nervous System 10: 115-120, 1973.
22. Gilbert F, Balaban G, Moorhead P, Bianchi D and Schlesinger H: Abnormalities of chromosome 1p in human neuroblastoma tumors and cell lines. Cancer Genet Cytogenet 7: 33-42, 1982.
23. Tumilowicz JJ, Nichols WW, Cholon JJ and Greene AE: Definition of a continuous human cell line derived from neuroblastoma. Cancer Res 30: 2110-2118, 1970.
24. Schlesinger HR, Gerson JM, Moorhead PS, Maguire H and Hummeler K: Establishment and characterization of human neuroblastoma cell lines. Cancer Res 36: 3094-3100, 1976.
25. Yoshihara T, Ikushima S, Hibi S, Misawa S and Imashuku S: Establishment and characterization of a human neuroblastoma cell line derived from a brain metastatic lesion. Hum Cell 6: 210-217, 1993.
26. Biedler JL, Helson L and Spengler BA: Morphology and growth, tumorigenicity, and cytogenetics of human neuroblastoma cells in continuous culture. Cancer Res 33: 2643-2652, 1973.

Oncogene (2010) 29, 2681–2690

www.nature.com/onc

ORIGINAL ARTICLE

Bmi1 is a MYCN target gene that regulates tumorigenesis through repression of *KIF1Bβ* and *TSLC1* in neuroblastoma

H Ochiai[1,2], H Takenobu[1], A Nakagawa[3], Y Yamaguchi[1], M Kimura[1], M Ohira[4], Y Okimoto[5], Y Fujimura[6], H Koseki[6], Y Kohno[2], A Nakagawara[7] and T Kamijo[1]

[1]Division of Biochemistry and Molecular Carcinogenesis, Chiba Cancer Center Research Institute, Chiba, Japan; [2]Department of Pediatrics, Graduate School of Medicine, Chiba University, Chiba, Japan; [3]Department of Pathology, National Center for Child Health and Development, Tokyo, Japan; [4]Laboratory of Cancer Genomics, Chiba Cancer Center Research Institute, Chiba, Japan; [5]Department of Hematology and Oncology, Chiba Children's Hospital, Chiba, Japan; [6]Developmental Genetics Group, RIKEN Research Center for Allergy and Immunology, Yokohama, Japan and [7]Division of Innovative Cancer Therapeutics, Chiba Cancer Center Research Institute, Chiba, Japan

Recent advances in neuroblastoma (NB) research addressed that epigenetic alterations such as hypermethylation of promoter sequences, with consequent silencing of tumor-suppressor genes, can have significant roles in the tumorigenesis of NB. However, the exact role of epigenetic alterations, except for DNA hypermethylation, remains to be elucidated in NB research. In this paper, we clarified the direct binding of MYCN to Bmi1 promoter and upregulation of Bmi1 transcription by MYCN. Mutation introduction into an MYCN binding site in the Bmi1 promoter suggests that MYCN has more important roles in the transcription of Bmi1 than E2F-related Bmi1 regulation. A correlation between MYCN and polycomb protein Bmi1 expression was observed in primary NB tumors. Expression of Bmi1 resulted in the acceleration of proliferation and colony formation in NB cells. Bmi1-related inhibition of NB cell differentiation was confirmed by neurite extension assay and analysis of differentiation marker molecules. Intriguingly, the above-mentioned Bmi1-related regulation of the NB cell phenotype seems not to be mediated only by p14ARF/p16INK4a in NB cells. Expression profiling analysis using a tumor-specific cDNA microarray addressed the Bmi1-dependent repression of *KIF1Bβ* and *TSLC1*, which have important roles in predicting the prognosis of NB. Chromatin immunoprecipitation assay showed that *KIF1Bβ* and *TSLC1* are direct targets of Bmi1 in NB cells. These findings suggest that MYCN induces Bmi1 expression, resulting in the repression of tumor suppressors through Polycomb group gene-mediated epigenetic chromosome modification. NB cell proliferation and differentiation seem to be partially dependent on the MYCN/Bmi1/tumor-suppressor pathways.
Oncogene (2010) **29**, 2681–2690; doi:10.1038/onc.2010.22; published online 1 March 2010

Correspondence: Professor T Kamijo, Division of Biochemistry and Molecular Carcinogenesis, Chiba Cancer Center Research Institute, 666-2 Nitona, Chuo-ku, Chiba 260-8717, Japan.
E-mail: tkamijo@chiba-cc.jp
Received 27 August 2009; revised 19 November 2009; accepted 4 January 2010; published online 1 March 2010

Keywords: Bmi1; MYCN; neuroblastoma; TSLC1; KIF1Bβ

Introduction

In tumorigenesis, besides the well-known genetic changes that occur in cancer, such as the deletion of tumor-suppressor genes (TSGs), amplification/activation of oncogenes and loss of heterozygosity or gene mutations in tumor-associated genes (Hanahan and Weinberg, 2000), epigenetic alterations, such as altered DNA methylation, misregulation of chromatin remodeling by histone modifications and aberrant expression of Polycomb group genes (PcGs) proteins have emerged as common hallmarks of many cancers (Jones and Baylin, 2002; Sparmann and van Lohuizen, 2006; Esteller, 2007; Rajasekhar and Begemann, 2007). PcGs are usually considered to be transcriptional repressors that are required for maintaining the correct spatial and temporal expressions of homeotic genes during development. (Schwartz and Pirrotta, 2008). Recent biochemical approaches have established that PcG proteins form multiprotein complexes, known as Polycomb-Repressive Complexes (PRCs). PRC2 contain Ezh2, EED, Suz12 and RbAp48, whereas the PRC1 complex consists of >10 subunits, including the oncoprotein Bmi1 and the HPC proteins, namely HPH1-3, RING1-2 and SCML (Rajasekhar and Begemann, 2007). In addition to being essential regulators of embryonic development, PcGs have also emerged as key players in the maintenance of adult stem cell populations (Valk-Lingbeek *et al.*, 2004; Pietersen and van Lohuizen, 2008). For example, Bmi1 is required for the self-renewal of hematopoietic and neural stem cells (Lessard and Sauvageau, 2003; Molofsky *et al.*, 2003, Iwama *et al.*, 2004), whereas the overexpression of EZH2 prevents hematopoietic stem cell exhaustion (Kamminga *et al.*, 2005). Consistent with their critical roles in development, differentiation and stem cell renewal, several PcGs are oncogenes, overexpressed in both solid and hematopoietic cancers (Valk-Lingbeek *et al.*, 2004; Rajasekhar and Begemann, 2007).

Neuroblastoma (NB) is one of the most common malignant solid tumors occurring in infancy and childhood and accounts for 10% of all pediatric cancers (Westemann and Schwab, 2002). NBs are derived from sympathetic neuroblasts with various clinical outcomes from spontaneous regression, caused by neuronal differentiation and/or apoptotic cell death, to malignant progression. Extensive cytogenetic and molecular genetic studies identified that genetic abnormalities, such as loss of the short arm of chromosome 1 (1p), amplification of *MYCN* and 17q gain, are frequently observed and often associated with poor clinical outcome (Brodeur *et al.*, 1984; Caron, 1995). Although numerous genetic abnormalities, including *MYCN* amplification, are involved in the development and/or progression of NB, the molecular mechanisms responsible for the pathogenesis of aggressive NB remain unclear. Epigenetic alterations, such as hypermethylation of promoter sequences, with consequent silencing of TSGs, such as *CASP8*, *RASSF1A*, *CD44*, *TSP-1* and *PTGER2*, can have significant roles in the tumorigenesis of NB (Teitz *et al.*, 2000; Yan *et al.*, 2003; Yang *et al.*, 2003, 2004; Sugino *et al.*, 2007). However, it was reported that the expression of several tumor-suppressor candidate genes, such as KIF1Bβ and TSLC1, is suppressed in NB cells, but the percentage of pathological mutations and promoter methylation in NB tumors was not so high (Ando *et al.*, 2008; Munirajan *et al.*, 2008). For the promoter DNA methylation-independent gene repression, the PcG complex might have a role in NB cell proliferation and differentiation, although the exact role of PcG in NB tumorigenesis remains to be elucidated. Regarding Bmi1 regulation in NB, the binding of E2F-1 to Bmi1 promoter and its activation were reported, and a strong expression of Bmi1 was observed in primary NBs (Nowak *et al.*, 2006). However, Bmi1 expression was not evaluated according to patient prognosis, and there was no correlation between *MYCN* amplification and Bmi1 expression in the report. Another group reported that Bmi1 suppression by knockdown induced several differentiation marker proteins, and impaired colony formation and tumor formation in immunodeficient mice, although Bmi1 overexpression in NB cells could not function as an oncogene (Cui *et al.*, 2006, 2007).

In this paper, we found that MYCN directly bound to Bmi1 promoter and induced its transcription. A correlation between MYCN and Bmi1 expressions was observed in both NB cell lines and primary tumors. The expression of Bmi1 in NB cells resulted in the upregulation of proliferation and colony formation; expression profiling using a tumor-specific cDNA microarray (Ohira *et al.*, 2005) addressed the Bmi1-dependent repression of TSGs, which has an important role in predicting the prognosis of NB.

Results

Bmi1 expression correlates with MYCN expression in NB cell lines and tumor samples

First, we studied Bmi1 expression by western blotting and found that the PRC1 complex protein Bmi1 and Ring1b expressions correlated with MYCN protein expression in NB cell lines, except for SK-N-AS cells (Figure 1Aa). At the mRNA level, we observed Bmi1 upregulation in *MYCN*-amplified SK-N-DZ to IMR32 cells (Figure 1Ab). Furthermore, the Bmi1 expression in primary NB specimens was clearly detected in the nucleus of *MYCN*-amplified NBs compared with those of *MYCN* single-copy NBs (Supplementary Figure S1), which was confirmed by statistical analysis (Figure 1B).

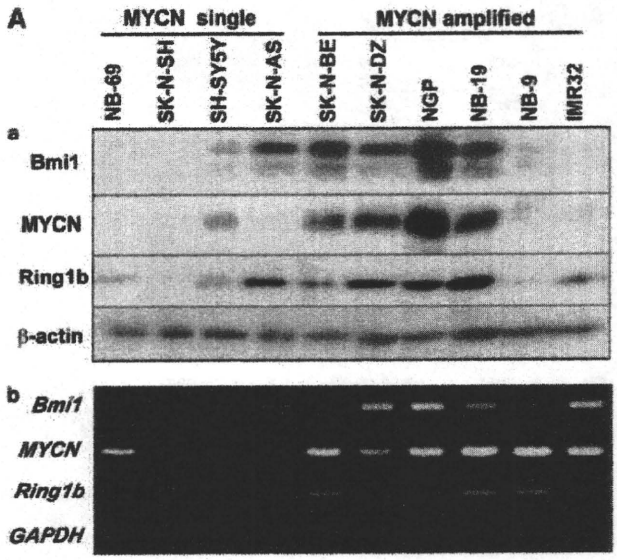

B

MYCN	Bmi1 Nuc (+)	Bmi1 Nuc (-)
single	0	10
amplified	5	1

Fisher's exact probability test
P<0.01

Figure 1 Bmi1 expression correlates with MYCN in NB (**A**). Bmi1 expression in NB cell lines. Western blotting analysis (a) and semi-quantitative RT–PCR (b) of Bmi1, Ring1b and MYCN were performed as described in the 'Materials and methods' section. (**B**) Immunohistochemical analysis of Bmi1 in NB tumor samples. In all, 10 *MYCN* single-copy NBs and 6 amplified NBs were analyzed. Statistical significance was determined by Fisher's exact probability test.

Bmi1 transcription is induced by MYCN

The above findings prompted us to study whether Bmi1 transcription is induced by MYCN in NB cells. We used Tet21/N cells expressing MYCN under the control of tetracycline (Lutz *et al.*, 1996). Four hours after tetracycline withdrawal, Bmi1 and Ring1b expressions were considerably increased along with MYCN induction both at mRNA and protein levels (Figure 2A a,b) associated with MYCN induction.

Using *in silico* analysis by the TFSEARCH program (http://www.cbrc.jp/research/db/TFSEARCHJ.html), we identified an MYCN binding site (E-box) at positions −181 and −764, −319 and −122 E2F binding

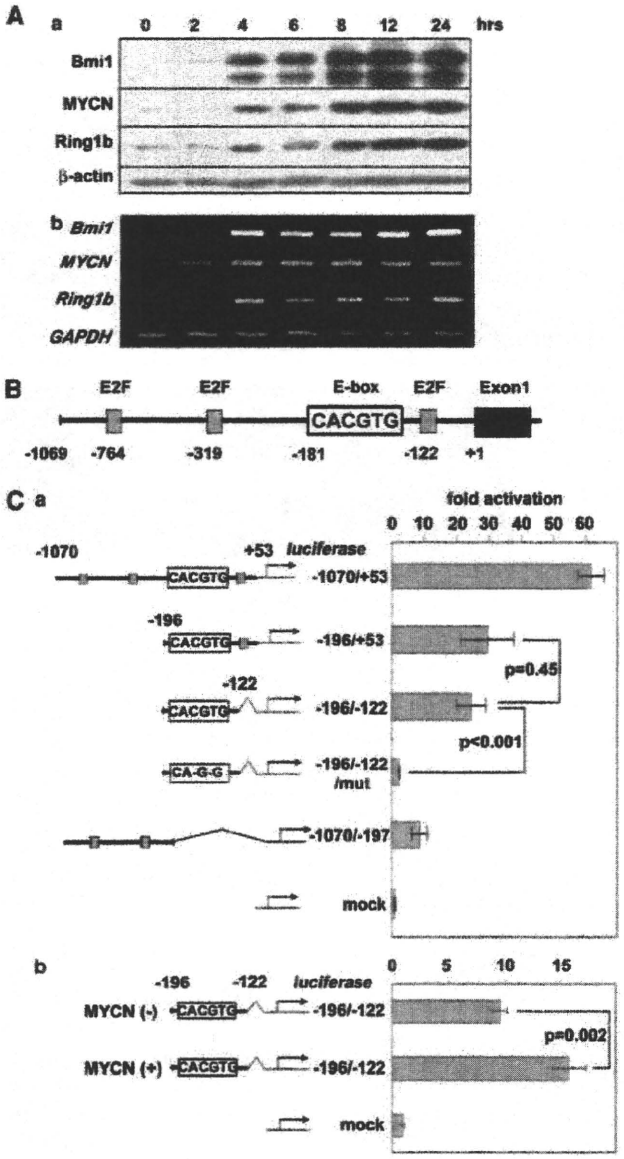

Figure 2 Bmi1 transcription is induced by MYCN. (**A**) Bmi1 expression was studied in MYCN-inducible Tet21/N cells. After withdrawal of tetracycline from culture medium, cells were collected at the indicated time points and analyzed by western blotting (Aa) and semi-quantitative RT–PCR (Ab). (**B**) Human Bmi1 promoter showing the locations (E2F sites and putative MYCN binding E-box) and sequence (putative MYCN binding E-box). Position +1 means the 5′ end of the RefSeq cDNA sequence (NM_005180). (**C**) MYCN activates Bmi1 through the binding site in the promoter. SK-N-DZ (*MYCN* amplified) and Tet21/N (MYCN-inducible) NB cells were transiently cotransfected with the indicated Bmi1 promoter-controlled reporter constructs. E2F site 1 and site 2 were deleted in the −196/+53 fragment; E2F sites 1–3 were deleted in the −196/−122 fragment. The results are representative of at least three independent experiments. Error bars represent the s.d. obtained with triplicate samples. Statistical significance was determined by the Mann–Whitney test.

sites in the human Bmi1 promoter (ENSG00000168283) (Figure 2B). To study the transcriptional regulation of Bmi1 expression in NB cells, initial transfection experiments were conducted with the Bmi1 luciferase/promoter reporter construct (−1070/+53), which contains the putative E-box element and E2F binding sites (Figure 2Ca); the −1070/+53 fragment showed significant promoter activity in an *MYCN*-amplified NB cell line SK-N-DZ. Deletion of −1070/−197 and −121/+53 still showed considerable activity (Figure 2Ca, activity of −196/+53 fragment compared with −196/−122), suggesting an important role of MYCN in Bmi1 promoter activity. Furthermore, this finding was confirmed by mutation of the E-box in the −196/−122 fragment (activity of −196/−122/mut).

Next, we studied the effect of MYCN on Bmi1 promoter activity using the MYCN-inducing NB cell line Tet21/N. MYCN induction significantly increased promoter activity in Tet21/N cells (Figure 2Cb). Intriguingly, we observed promoter activity even in MYCN (−) cells. We speculated that residual MYC (c-MYC) may contribute to activity in these cells (Supplementary Figure S2)

MYCN binds to the E-box region in Bmi1 promoter

To address whether MYCN could be recruited onto the E-box in Bmi1 promoter in NB cells, we performed chromatin immunoprecipitation (ChIP) assays by quantitative real-time PCR (qPCR). We found that MYCN binding to the Bmi1 promoter region was clearly detected in *MYCN*-amplified SK-N-DZ and NB-19 cells but not in *MYCN*-single SH-SY5Y cells (Figure 3a). Furthermore, this observation was confirmed in MYCN-inducible Tet21/N cells (Figure 3b), indicating that MYCN binds to the Bmi1 promoter region and has a considerable role in Bmi1 transcription in *MYCN*-amplified NB tumors.

Bmi1 regulates NB cell proliferation

Next, we examined the effect of Bmi1 on the cell growth of NB cells by exogenous expression of Bmi1. SH-SY5Y cells were infected with the mock virus and the FLAG-tagged Bmi1 expression virus. Cell growth was studied by the WST (water-soluble tetrazolium salt) assay and showed that Bmi1 significantly accelerated cell proliferation compared with mock cells (Figure 4a). In the soft agar assay, Bmi1-expressing SH-SY5Y cells formed anchorage-independent colonies effectively, although colony formation was hardly detectable in parental and mock cells (Figure 4b). Interestingly, Ring1b was increased in Bmi1-expressing SH-SY5Y cells (Figure 4c) and Tet21/N cells (Figure 4e); the well-known Bmi1 targets p14ARF and p16INK4a protein amounts were not markedly changed by Bmi1 expression, although mRNA expression was slightly suppressed in SH-SY5Y cells. These results suggest that increased PRC1-mediated gene repression, except for p14ARF and p16INK4a, might have an important role in NB cells. In addition, we found an additive effect of MYCN induction in Bmi1-expressing Tet21/N cells, suggesting the significance of MYCN targets, except for Bmi1, in NB cell proliferation. Bmi1 knockdown by lentivirus-mediated shRNA transduction strongly inhibited cell

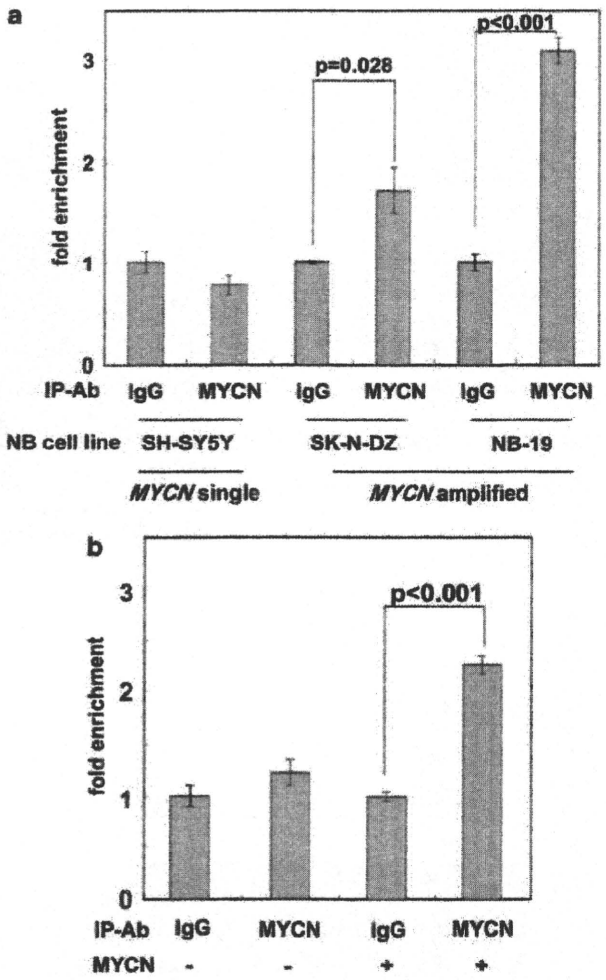

Figure 3 MYCN binds to human Bmi1 promoter *in vivo*. Cross-linked chromatin was isolated from SH-SY5Y (*MYCN* single copy, **a**), SK-N-DZ and NB-19 (*MYCN* amplified, panel a) and Tet21/N (MYCN-inducible, **b**) NB cells. Immunoprecipitation was performed with an anti-MYCN antibody (clone NCM II 100) or control IgG. The precipitated chromatin was used as templates for qPCR analysis as described in the 'Materials and methods' section. In panel b experiments, Tet21/N were cultured in the condition of either tet-off (MYCN (+)) or tet-on (MYCN (−)). The results are representative of at least three independent experiments. Error bars represent the s.d. obtained with triplicate samples. Statistical significance was determined by the Mann–Whitney test.

Figure 4 Bmi1 effects on NB cell proliferation. WST assay (**a**) and soft agar colony formation assay (**b**) of Bmi1-expressing NB cells (SH-SY5Y). The results are representative of at least three independent experiments. Error bars represent the s.d. obtained with triplicate samples. (**c**) Western blotting (left panel) and semi-quantitative RT–PCR assay (right panel) of Bmi1-expressing SH-SY5Y cells. Analyzed molecules are shown in the left margin of the panels. (**d**) Soft agar colony formation assay of Bmi1-expressing NB cells (Tet21/N). Tet21/N cells were infected with either mock lentivirus (Bmi1 (−)) or Bmi1-expressing lentivirus (Bmi1 (+)), and cultured with either Tet(−) (MYCN+) or Tet(+) (MYCN−) complete soft agar media. The results are representative of at least three independent experiments. Error bars represent the s.d. obtained with triplicate samples. Statistical significance was determined by the Mann–Whitney test. (**e**) Western blotting (left panel) and semi-quantitative RT-PCR assay (right panel) of Tet21/N cells treated as described above. Analyzed molecules are shown in the left margin of the panels.

proliferation in several NB cell lines, such as SK-N-AS, IMR32, TGW, etc. (Supplementary Figure S3 and data not shown), consistent with previous reports (Cui *et al.*, 2006).

Bmi1 controls NB cell differentiation

Treatment with TPA (12-*O*-tetradecanoylphorbol 13-acetate) or ATRA (all-trans-retinoic acid) effectively

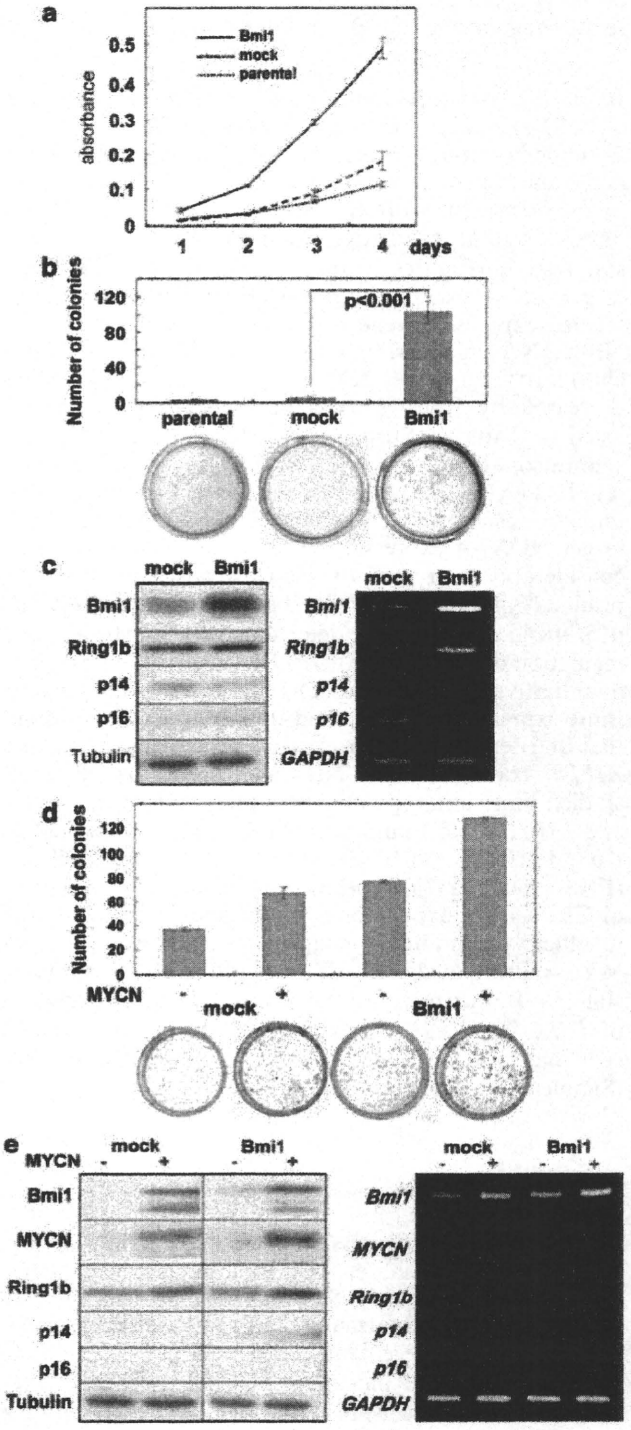

induced NB cell differentiation, for example, neurite extension (Figure 5Aa), and the expression of differentiation markers (Figure 5Ab and c). Interestingly, Bmi1 was downregulated at the protein level along with NB cell differentiation by TPA or ATRA treatment. To address the role of Bmi1 in NB cell differentiation, we knocked down Bmi1 using shRNA-expressing lentivirus. Intriguingly, only Bmi1 knockdown induced significant neurite extension (Figure 5Ba) and the expression of differentiation markers GAP43 and NF68 (Figure 5Bc), suggesting the existence of Bmi1-related regulation of NB cell differentiation.

Bmi1 binds to the promoter region of TSGs TSLC1 and KIF1Bβ and suppresses transcription in NB cells

To understand how Bmi1 controls NB cell proliferation and tumorigenesis, we chose to identify their target genes, except for p14ARF/p16INK4a, as we could not observe significant changes in these well-known tumor suppressors (Figures 4 and 5). To identify the Bmi1 target genes, except for p14ARF and p16INK4a, we studied expression gene profiling using an appropriate NB cDNA microarray (named the CCC-NHR13000 chip) carrying 13 440 cDNA spots. The top 10 genes decreased by Bmi1 expression in SK-N-BE cells are listed in Table 1. Surprisingly, the well-known tumor suppressors (TSGs) in NB TSLC1 (NM_014333.3) and KIF1Bβ (AB017133) are ranked as the first and second targets, respectively. The previously reported Bmi1 target HOXA4 expression (Cao *et al.*, 2005) was also considerably repressed by Bmi1. Consistent with our results (Figures 4 and 5), the ranking of p14ARF/p16INK4a was 5258. We determined the Bmi1-mediated regulation of *TSLC1* and *KIF1Bβ* transcription by semi-quantitative real-time (RT)-PCR experiments using Bmi1-expressing and knocked-down NB cells and found that Bmi1 expression considerably repressed *TSLC1* and *KIF1Bβ* transcription in NB cells (Figure 6a). Next, we studied Bmi1 binding to the promoter regions of *TSLC1* and *KIF1Bβ* and found that Bmi1 specifically bound to the KIF1Bβ (ENSG00000054523) and TSLC1 (ENSG00000105767) promoter region in NB cells. qPCR ChIP expressions confirmed Bmi1 binding to these promoters, suggesting the existence of MYCN/Bmi1-mediated *TSLC1* and *KIF1Bβ* suppression in NB. Furthermore, this Bmi1-mediated regulation of *TSLC1* and *KIF1Bβ* expression was not only in NB cells but also in squamous lung cancer QG56 cells (Supplementary Figure S4).

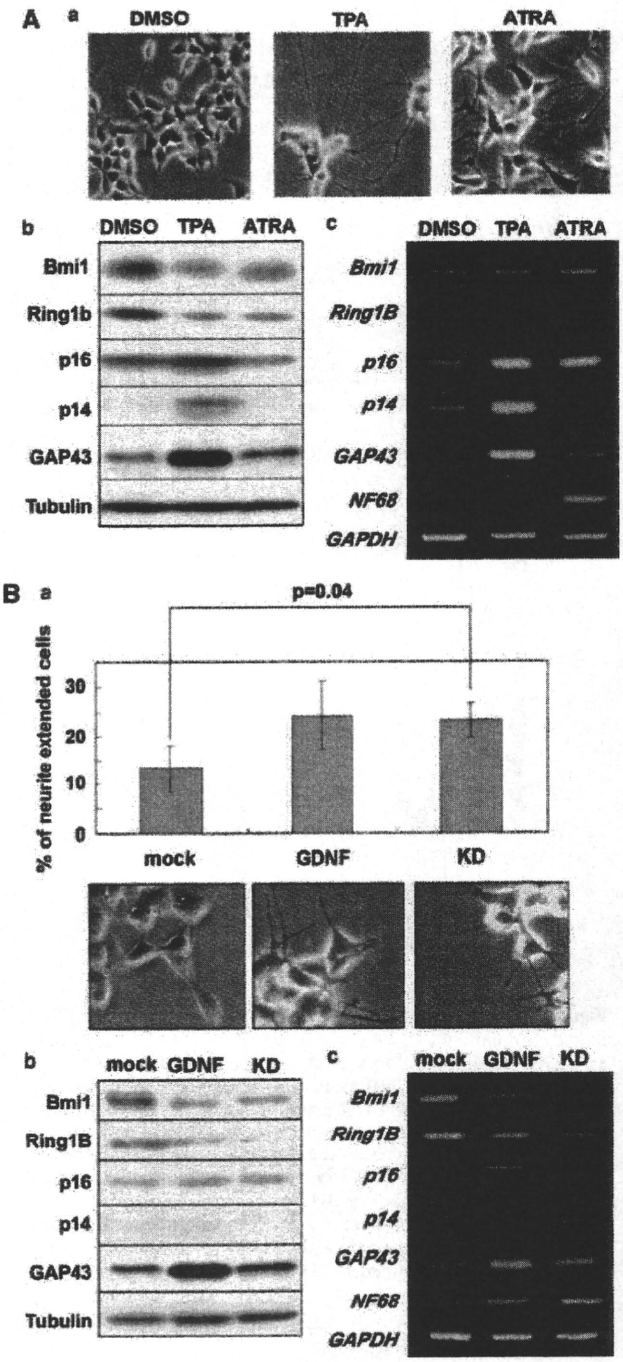

Figure 5 Bmi1 regulates NB cell differentiation. (**A**) TGW cells were treated with 0.1% DMSO, 100 nM of 12-*O*-tetradecanoylphorbol-13-acetate (TPA) and 5 μM all-trans-retinoic acid (RA) for 72 h. Neurite extension (a) was analyzed as described in the 'Materials and methods' section, and the indicated molecule expression was studied by western blotting analysis (b) and semi-quantitative RT–PCR assay (c). (**B**) TGW cells were infected with either mock- or Bmi1-knockdown lentivirus, as described in the 'Materials and methods' section. Neurite extension was assayed using mock-infected (left), mock-infected 10 ng/ml GDNF (middle) and Bmi1-knocked down (right) TGW cells. The results are representative of at least three independent experiments. Error bars represent the s.d. obtained with triplicate samples. Statistical significance was determined by the Mann–Whitney test. We could not detect NF68 expression at the protein level.

Discussion

Bmi1 regulates the expression of TSGs in NB

Among the PcG target genes in cancer cells, PcG-mediated repression of TSGs has an indispensable role in tumorigenesis (Sparmann and van Lohuizen, 2006; Rajasekhar and Begemann, 2007). As a result of PcG overexpression, the increased PRC1/PRC2 complexes bind to PcG target gene promoter lesions. Next, putative

Table 1 Top 10 genes suppressed by Bmi1 in NB cells

Rank	*Gene name*	*Symbol*	*Accession*	*Fold induction (log(Bmi1)/log(GFP))*
1	KIF1B	KIF1B	AB011163	−2.961
2	TSLC1	TSLC1	NM_014333	−1.469
3	CHGA	CHGA	NM_001275	−1.296
4	DBH	DBH	NM_000787	−1.263
5	WKID22370	ARCN1	NM_001655	−1.206
6	WKID02790	KIAA0970	NM_014949	−1.184
7	FHL1	FHL1	NM_001449	−1.167
8	WKID21762	TMP21	NM_006827	−1.121
9	Nbla20566	RISC	NM_021626	−1.105
10	WKID00168	ENO1	NM_001428	−1.097
757	HOXA4	HOXA4	NM_002141	−0.439
1528	P15_CDKN2B	CDKN2B	NM_004936	−0.314
5258	P16_P14CDKN2A	CDKN2A	NM_000077	−0.009

Abbreviation: NB, neuroblastoma.
Bmi1 was overexpressed by lentivirus-mediated transduction in SK-N-BE cells. Total RNA was extracted and subjected to expression profiling analysis by an appropriate NB cDNA microarray as described in the 'Materials and methods' section. The results are the averages of at least three experiments and the top 10 genes suppressed are presented. Overall, 11 293 genes were analyzed. We will inform the microarray data if there is a request.

PRC/DNA methyltransferase cross talk seems to induce aberrant DNA methylation as PRC2 member EZH2 was shown to recruit DNA methyltransferase to select target genes (Viré *et al.*, 2006). In fact, PcG protein target genes have been found to display a greater likelihood of acquiring specific promoter DNA hypermethylation during cancer progression than nontarget genes (Iwama *et al.*, 2004; Kamminga and de Haan, 2006). It is interesting that the *p16INK4a-p14ARF* locus represents one of the above-identified candidates with PRCs binding and hyper DNA methylation in the promoters in cancer cells. This locus encodes two alternatively spliced gene products, the tumor-suppressor protein p16INK4a (an inhibitor of cell-cycle progression) and p14ARF (a regulator of p53) (Sherr, 2004). Bmi1 is a well-known repressor of p16INK4a and, in some cases, such as in mammalian cells, p14ARF genes (Jacobs *et al.*, 1999; Molofsky *et al.*, 2006). However, several previous reports have indicated that there could be another important Bmi1 target gene, especially in the nervous system, in addition to p16INK4a/p14ARF (Jacobs *et al.*, 1999; Bruggeman *et al.*, 2007).

In our study, Bmi1 overexpression accelerated the proliferation of several NB cell lines, although p14ARF/p16INK4a repression was not so obvious (Figure 4). Furthermore, it was previously reported that the probability of p16INK4a inactivation in NB was not high (Easton *et al.*, 1998). These results prompted us to screen Bmi1-dependent gene repression using a tumor-specific cDNA microarray, and we identified the repression of TSGs, *KIF1Bβ* and *TSLC1* (Table 1). This repression was confirmed by semi-quantitative RT-PCR experiments, and the *in vivo* binding of Bmi1 to these promoters was addressed by ChIP assay with qPCR using Bmi1-overexpressing NB cells (Figure 6). Accumulating lines of evidence strongly suggest that downregulation of TSLC1 in various cancers, including lung cancer, hepatocellular carcinoma, gastric cancer, pancreatic adenocarcinoma, prostate cancer, breast cancer, nasopharyngeal carcinoma and cervical cancer, might be due to the hypermethylation of its promoter region (Murakami, 2005). In sharp contrast to these cancers, we did not detect hypermethylation of the promoter region of the *TSLC1* gene in primary NBs or NB-derived cell lines, and *TSLC1* expression levels significantly correlated with the stage, Shimada's pathological classification and *MYCN* amplification status (Ando *et al.*, 2008). We also found that *KIF1Bβ*, located at chromosome 1p36.2, was significantly suppressed in *MYCN*-amplified NB samples, although its mutation rate was not high and promoter hypermethylation was not observed (Munirajan *et al.*, 2008). Furthermore, a previous report mentioned that a cluster of genes located in 1p36, including *KIF1Bβ*, is downregulated in NBs with poor prognosis, but was not due to CpG island methylation (Carén *et al.*, 2005). Taken together, it suggests that MYCN-induced Bmi1 suppresses several TSGs by their promoter silencing and contributes to NB tumorigenesis. Systematic analysis of PcG binding to gene promoter lesions will be required for the study of epigenetic regulation of tumorigenesis-related gene expression in NB.

Regulation of Bmi1 gene transcription

Despite these important functions in development and tumorigenesis, little is known about transcriptional regulation of the *Bmi1* gene. The transcription factors known to regulate Bmi1 expression are sonic hedgehog-activated Gli1 protein (Leung *et al.*, 2004), E2F family members (Nowak *et al.*, 2006), zinc-finger transcription factor SALL4 (Yang J *et al.*, 2007) and c-Myc (Guney *et al.*, 2006). As E2F1 regulates NB tumorigenesis through direct binding to *MYCN* promoter and its activation, E2F may regulate NB cells using complicated MYCN, MYCN/Bmi1 and Bmi1 regulation mechanisms (Strieder and Lutz, 2003; Kramps *et al.*, 2004).

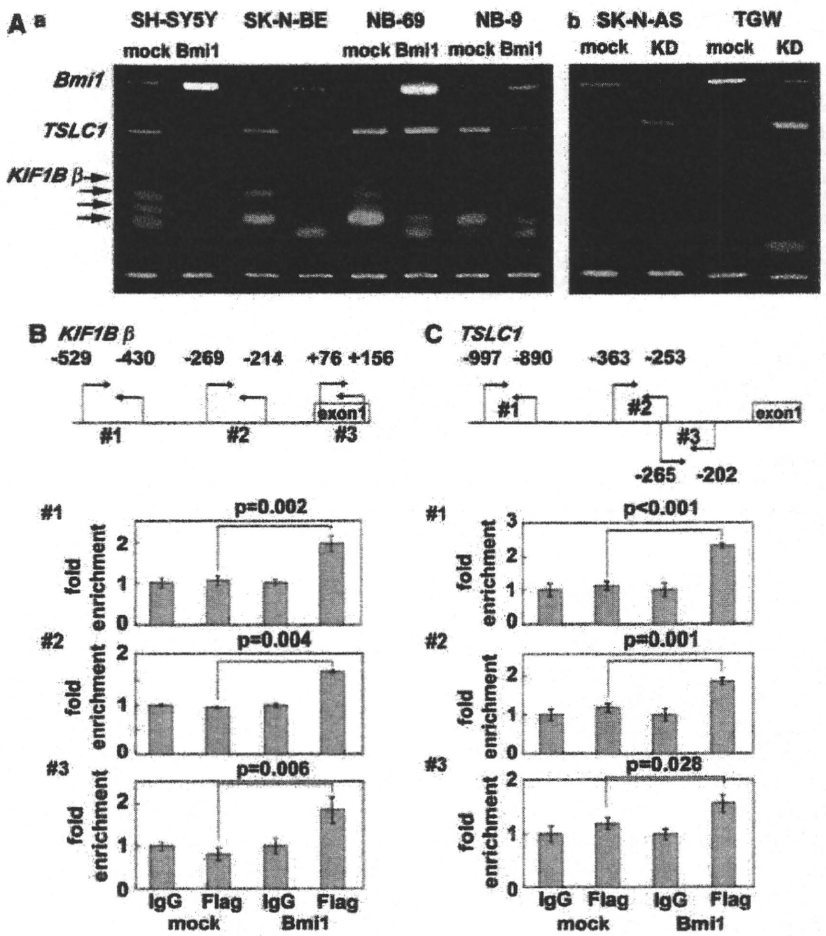

Figure 6 Bmi1 directly binds to TSLC1 and KIF1Bβ promoters and represses transcription in NB cells. (**A**) The indicated NB cell lines were infected with Bmi1-expressing lentivirus (a) and Bmi1-shRNA lentivirus (b), as described in the 'Materials and methods' section. Bmi1 expression modulated by lentivirus infection was examined (top lane of panels). TSLC1 and KIF1Bβ expressions were studied by semi-quantitative RT–PCR assay. The primer sequences are shown in Supplementary Table S1. The results are representative of at least three independent experiments. Arrows indicate alternative splicing products of KIF1Bβ (Munirajan *et al.*, 2008). (**B**: KIF1Bβ and **C**: TSLC1) SK-N-BE cells were infected with FLAG-Bmi1-expressing lentivirus and subjected to quantitative ChIP assay as described in the 'Materials and methods' section. Immunoprecipitation was performed by anti-FLAG (M2) antibody and control mouse IgG. The primers for qPCR analysis were designed using the Primer3 program (Applied Biosystems, Foster City, CA, USA) and locations are indicated in the diagrams. The primer sequences are shown in Supplementary Table S2. The results are presented as fold enrichment and are representative of at least three independent experiments. Error bars represent the s.d. obtained with triplicate samples. Statistical significance was determined by the Mann–Whitney test.

In this paper, we found that MYCN directly binds to the Bmi1 promoter *in vivo* and that binding is enhanced by *MYCN* amplification in NB cell lines and MYCN induction using tetracycline-withdrawal-based gene induction plasmid (Figure 3). MYCN expression correlates with Bmi1 levels both at mRNA and protein levels in NB cell lines (Figures 1A, 2a) and NB tumor samples (Figure 1b). Next, we studied the role of the MYCN binding site and several E2F binding sites in Bmi1 transcriptional regulation using a luciferase expression system (Figure 2). Intriguingly, we found that significantly high luciferase activities of E-box + E2F site promoter (Figure 2c, −196/ + 53 fragment) and E2F site deletion from this fragment (Figure 2c, −196/−122 fragment) resulted in only a modest reduction of activity. Furthermore, base-deleted mutation to the E-box almost completely suppressed the activity of the deltaE2F fragment (Figure 2c, −196/−122/mut), suggesting the role of MYCN in Bmi1 transcription. MYCN-dependent Bmi1 induction was observed not only in NB cell experiments but also in *in vivo* experiments. The Bmi1 mRNA level was higher in NBs occurring in tyrosine hydroxylase promoter-induced *MYCN* transgenic mice than in ganglions with hyperplasia and normal ganglion (S Kishida and K Kadomatsu, personal communication). Accordingly, these results suggest the important role of MYCN in Bmi1 transcription in NB and further studies will be required to address the exact mechanism of Bmi1 transcriptional regulation by E2F and/or MYCN.

Furthermore, the epigenetic regulation of Bmi1 transcription will be an interesting subject of NB research as we observed considerable effects of Bmi1 on other PRC complex proteins.

Taken together, we found an intriguing MYCN/Bmi1/tumor-suppressor pathway in NB cells. This pathway might have a remarkable impact on NB tumorigenesis and is considered a target for the development of molecular targeted therapy for therapy-resistant NBs.

Materials and methods

Cell culture

Human NB cell lines and QG56 human lung squamous carcinoma cells were obtained from official cell banks and were cultured in RPMI1640 or Dulbecco's modied Eagle's medium (Wako, Osaka, Japan) supplemented with 10% heat-inactivated fetal bovine serum (Invitrogen, Carlsbad, CA, USA) and 50 μg/ml penicillin/streptomycin (Sigma-Aldrich, St Louis, MO, USA) in an incubator with humidified air at 37 °C with 5% CO_2. Tet21/N cells, which are derived from the SH-EP NB cell line, express MYCN under the control of tetracycline (tet-off system) (kindly provided by Dr M Schwab; Lutz *et al.*, 1996). MYCN expression in Tet21/N cells was repressed by 100 ng/ml tetracycline (Sigma-Aldrich) for 48 h before each experiment.

Treatment of cell lines with glial cell line-derived neurotrophic factor, ATRA or TPA

TGW cells were seeded at a density of 1×10^5 cells per 6-cm diameter tissue culture dish in the presence of glial cell line-derived neurotrophic factor (Invitrogen), ATRA (Sigma-Aldrich) or TPA (Nacalai Tesque, Kyoto, Japan) at the concentrations indicated in figure legends, and then the cells were grown for 3 days.

Cell proliferation assay

NB cells were seeded in 96-well plates at a density of 10^3 cells per well in a final volume of 100 μl. The culture was maintained under 5% CO_2 and 10 μl WST-8 labeling solution (Cell counting Kit-8; DOJINDO, Kumamoto, Japan) was added, and the cells were returned to the incubator for 2 h. The absorbance of the formazan product formed was detected at 450 nm in a 96-well spectrophotometric plate reader, according to the manufacturer's protocol.

Western blot analysis

The cells were lysed in a buffer containing 5 mM EDTA, 2 mM Tris–HCl (pH 7.5), 10 mM β-glycerophosphate, 5 μg/ml aprotinin, 2 mM phenylmethylsulfonyl fluoride, 1 mM Na_3VO_4, protease inhibitor cocktail (Nacalai Tesque) and 1% SDS. Western blot analysis was performed as previously reported (Kurata *et al.*, 2008). After transferring to an Immobilon-P membrane (Millipore, Bedford, MA, USA), proteins were reacted with either anti-Bmi1 mouse monoclonal (229F6; Upstate, Charlottesville, VA, USA), anti-MYCN rabbit polyclonal (C-19; Santa Cruz, Santa Cruz, CA, USA) p14 (14P02; Oncogene) mouse, p16 (16P04; Neomarkers/Labvision, Fremont, CA, USA) mouse, anti-β-actin (Sigma-Aldrich) or a monoclonal anti-tubulin (Neomarkers Labvision) antibody. Anti-Ring1b mouse monoclonal antibodies were as described in a previous report (Atsuta *et al.*, 2001).

Immunohistochemistry

A 4-μm thick section of formalin-fixed, paraffin-embedded tissues was stained with hematoxylin and eosin and the adjacent sections were immunostained for Bmi1 using a polyclonal anti-Bmi1 antibody (AP2513c; ABGENT, San Diego, CA, USA). The Bench-Mark XT immunostainer (Ventana Medical Systems, Tucson, AZ, USA) and 3-3′ diaminobenzidine detection kit (Ventana Medical Systems) were used for visualization. Appropriate positive and negative control staining was also performed in parallel for each immunostaining. The tumor samples used in this study were kindly provided from various institutions and hospitals in Japan. Informed consent was obtained at each institution and hospital. All tumors were diagnosed clinically and pathologically as NBs and *MYCN* copy number was determined as previously described (Kurata *et al.*, 2008).

Semi-quantitative RT–PCR

The methods of semi-quantitative RT–PCR analysis were previously described (Kurata *et al.*, 2008). Total cellular RNA to prepare RT–PCR templates was extracted from NB cell lines using Isogen (Nippon Gene K K, Tokyo, Japan), and cDNA was synthesized from 1 μg total RNA templates according to the manufacturer's protocol (RiverTra-Ace-α RT–PCR kit; TOYOBO, Osaka, Japan). Primer sequences are described in Supplementary Table S1.

qPCR analysis for ChIP assay

qPCR analysis was performed using the ABI PRISM 7500 Real-Time PCR System (Applied Biosystems, Foster City, CA, USA), according to the manufacturer's instructions using SYBR Premix Dimer Eraser (Takara Bio, Ohtsu, Shiga, Japan). The primers for qPCR were designed and synthesized to produce 50–150 bp products. The primer sequence is listed in Supplementary Table S2. Each sample was amplified in triplicate. In Figure 3, the primer set was designed in E-box upstream of Bmi1 (Bmi1 promoter 1). In Figures 3, 6b, primer sets were designed in KIF1Bβ (KIF1B promoter 1, 2, 3) and TSLC1 (TSLC1 promoters 1, 2, 3).

Lentiviral infection

The packaging cell line HEK 293T (4×10^6) was plated and transfected the next day, when 1.5 μg of the transducing vectors containing the gene or shRNA, and 2.0 μg of the packaging vectors (Sigma-Aldrich) were cotransfected by the Fugene6 transfection reagent (Roche Applied Science, Indianapolis, IN, USA) according to the manufacturer's protocol. The medium was changed the next day and cells were cultured for another 24 h. Conditioned medium was then collected and cleared of debris by filtering through a 0.45-μm filter (Millipore). Thereafter, 1×10^5 NB cells were seeded in each well of a 6-well plate, and transduced by lentiviral-conditioned media. Transduced cells were analyzed by western blotting and RT–PCR.

Overexpression and knockdown of Bmi1

For the overexpression of Bmi1, FLAG-tagged mBmi1 plasmid was subcloned into lentivirus vector pHR-SIN-DL1. Cells were cultured in RPMI1640 and pooled. The pLKO.1-puromycin-based lentiviral vectors containing five sequence-verified shRNAs targeting human Bmi1 (RefSeq NM_005180) were obtained from the MISSION TRC-Hs 1.0 (Human) shRNA library (Sigma-Aldrich). Virus production, infection and selection were performed according to the manufacturer's protocol. At 1 week post infection, cells

were harvested and knockdown efficiency was assessed by western blotting. We checked Bmi1 knockdown by the five lentivirus-produced shRNAs and used two for experiments.

Luciferase reporter assay

The −1070/+53, −196/+53, −196/−122, −196/−122/mut (E-box sequence CACGTG changed to CA-G-G), −1070/+53 5′-upstream fragments were subcloned into luciferase reporter plasmid pGL4.17 (luc2/Neo) Luciferase Reporter Vector (Promega, Madison, WI, USA).

Tet21/N and SK-N-DZ cells were seeded in a 12-well plate 24 h before transfection at a concentration of 5×10^4 cells per well. Cells were cotransfected with Renilla luciferase reporter plasmid (pRL-TK, 10 ng) and luciferase reporter plasmid with the 5′-upstream region of the Bmi1 gene. The total amount of plasmid DNA per transfection was kept constant (510 ng) with pBlueScript KS+ by Lipofectamine 2000 (Invitrogen). At 48 h after transfection, cells were lysed and their luciferase activities were measured by the Dual-Luciferase reporter system (Promega). The rey luminescence signal was normalized on the basis of the Renilla luminescence signal.

ChIP assay

ChIP assay was performed as described previously (Orlando *et al*., 1997, Fujimura *et al*., 2006). Cross-linked chromatin prepared from the indicated cells was precipitated with normal mouse IgG (eBioscience, San Diego, CA, USA), monoclonal anti-MYCN antibody (NCMII100; Calbiochem, San Diego, CA, USA) or anti-Flag antibody (M2; Sigma-Aldrich). 'Input' DNA was isolated from the initial lysates of genomic DNA. Species-matched immunoglobulin-immunoprecipitated DNA (IgG), derived from the same volume of the chromatin fraction used for specific antibody immunoprecipitation, was subjected to PCR. Primers used in this study are listed in Supplementary Table S2. Each series of experiments was conducted at least three times.

cDNA microarray experiments

For gene expression profiling, in-house cDNA microarray with 13 440 spots was used. In all, 10 μg each of total RNA were labeled with the CyScribe RNA labeling kit in accordance with the manufacturer's manual (GE healthcare, Little Chalfont, Buckinghamshire, UK), followed by probe purification using the Qiagen MinElute PCR purification kit (Qiagen, Valencia, CA, USA). We used a mixture of RNAs isolated from eight human adult cancer cell lines as a common reference. RNAs from Bmi1-infected SK-N-BE and mock-infected SK-N-BE cells were labeled with Cy3 dye and a reference RNA mixture was labeled with Cy5 dye, mixed, and used as probes together with yeast tRNA and polyA for suppression. Subsequent hybridization and washing were conducted as described previously (Ohira *et al*., 2005). Hybridized microarrays were scanned using the Agilent G2505A confocal laser scanner (Agilent technology, Santa Clara, CA, USA), and fluorescent intensities were quantified using the GenePix Pro microarray analysis software (Axon Instrument, Foster City, CA, USA). The resulting relative expression values for the gene spots were compared between Bmi1-infected and mock-infected SK-N-BE cells

Conflict of interest

The authors declare no conflict of interest.

Acknowledgements

We thank K Sakurai for technical assistance, and Daniel Mrozek, Medical English Service, for editorial assistance. This study was supported in part by a grant-in-aid from the Sankyo Foundation of Life Science, a grant-in-aid from the Ministry of Health, Labor, and Welfare for Third Term Comprehensive Control Research for Cancer, a grant-in-aid for Cancer Research (20–13) from the Ministry of Health, Labor, and Welfare of Japan, and a grant-in-aid from the Ministry of Education, Culture, Sports, Science and Technology, Japan.

References

Ando K, Ohira M, Ozaki T, Nakagawa A, Akazawa K, Suenaga Y *et al*. (2008). Expression of TSLC1, a candidate tumor suppressor gene mapped to chromosome 11q23, is downregulated in unfavorable neuroblastoma without promoter hypermethylation. *Int J Cancer* **123**: 2087–2094.

Atsuta T, Fujimura S, Moriya H, Vidal M, Akasaka T, Koseki H. (2001). Production of monoclonal antibodies against mammalian Ring1B proteins. *Hybridoma* **20**: 43–46.

Brodeur GM, Seeger RC, Schwab M, Varmus HE, Bishop JM. (1984). Amplification of N-myc in untreated human neuroblastomas correlates with advanced disease stage. *Science* **224**: 1121–1124.

Bruggeman SW, Hulsman D, Tanger E, Buckle T, Blom M, Zevenhoven J *et al*. (2007). Bmi1 controls tumor development in an Ink4a/Arf-independent manner in a mouse model for glioma. *Cancer Cell* **12**: 328–341.

Cao R, Tsukada Y, Zhang Y. (2005). Role of Bmi-1 and Ring1A in H2A ubiquitylation and Hox gene silencing. *Mol Cell* **20**: 845–854.

Caron H. (1995). Allelic loss of chromosome 1 and additional chromosome 17 material are both unfavourable prognostic markers in neuroblastoma. *Med Pediatr Oncol* **24**: 215–221.

Carén H, Ejeskär K, Fransson S, Hesson L, Latif F, Sjöberg RM *et al*. (2005). A cluster of genes located in 1p36 are down-regulated in neuroblastomas with poor prognosis, but not due to CpG island methylation. *Mol Cancer* **4**: 10.

Cui H, Ma J, Ding J, Li T, Alam G, Ding HF. (2006). Bmi-1 regulates the differentiation and clonogenic self-renewal of I-type neuroblastoma cells in a concentration-dependent manner. *J Biol Chem* **281**: 34696–34704.

Cui H, Hu B, Li T, Ma J, Alam G, Gunning WT *et al*. (2007). Bmi-1 is essential for the tumorigenicity of neuroblastoma cells. *Am J Pathol* **170**: 1370–1378.

Easton J, Wei T, Lahti JM, Kidd VJ. (1998). Disruption of the cyclin D/cyclin-dependent kinase/INK4/retinoblastoma protein regulatory pathway in human neuroblastoma. *Cancer Res* **58**: 2624–2632.

Esteller M. (2007). Cancer epigenomics: DNA methylomes and histone-modification maps. *Nat Rev Genet* **8**: 286–298.

Fujimura Y, Isono K, Vidal M, Endoh M, Kajita H, Mizutani-Koseki Y *et al*. (2006). Distinct roles of Polycomb group gene products in transcriptionally repressed and active domains of Hoxb8. *Development* **133**: 2371–2381.

Guney I, Wu S, Sedivy JM. (2006). Reduced c-Myc signaling triggers telomere-independent senescence by regulating Bmi-1 and p16(INK4a). *Proc Natl Acad Sci USA* **103**: 3645–3650.

Hanahan D, Weinberg RA. (2000). The hallmarks of cancer. *Cell* **100**: 57–70.

Iwama A, Oguro H, Negishi M, Kato Y, Morita Y, Tsukui H *et al.* (2004). Enhanced self-renewal of hematopoietic stem cells mediated by the polycomb gene product Bmi-1. *Immunity* **21**: 843–851.

Jacobs JJ, Kieboom K, Marino S, DePinho RA, van Lohuizen M. (1999). The oncogene and Polycomb-group gene bmi-1 regulates cell proliferation and senescence through the ink4a locus. *Nature* **397**: 164–168.

Jones PA, Baylin SB. (2002). The fundamental role of epigenetic events in cancer. *Nat Rev Genet* **3**: 415–428.

Kamminga LM, Bystrykh LV, de Boer A, Houwer S, Douma J, Weersing E *et al.* (2005). The Polycomb group gene Ezh2 prevents hematopoietic stem cell exhaustion. *Blood* **107**: 2170–2179.

Kamminga LM, de Haan G. (2006). Cellular memory and hematopoietic stem cell aging. *Stem Cells* **24**: 1143–1149.

Kramps C, Strieder V, Sapetschnig A, Suske G, Lutz W. (2004). E2F and Sp1/Sp3 synergize but are not sufficient to activate the *MYCN* gene in neuroblastomas. *J Biol Chem* **279**: 5110–5117.

Kurata K, Yanagisawa R, Ohira M, Kitagawa M, Nakagawara A, Kamijo T. (2008). Stress via p53 pathway causes apoptosis by mitochondrial Noxa upregulation in doxorubicin-treated neuroblastoma cells. *Oncogene* **27**: 741–754.

Lessard J, Sauvageau G. (2003). Bmi-1 determines the proliferative capacity of normal and leukaemic stem cells. *Nature* **423**: 255–260.

Leung C, Lingbeek M, Shakhova O, Liu J, Tanger E, Saremaslani P *et al.* (2004). Bmi1 is essential for cerebellar development and is overexpressed in human medulloblastomas. *Nature* **428**: 337–341.

Lutz W, Stohr M, Schurmann J, Wenzel A, Lohr A, Schwab M. (1996). Conditional expression of N-myc in human neuroblastoma cells increases expression of alpha-prothymosin and ornithine decarboxylase and accelerates progression into S-phase early after mitogenic stimulation of quiescent cells. *Oncogene* **13**: 803–812.

Molofsky AV, Pardal R, Iwashita T, Park IK, Clarke MF, Morrison SJ. (2003). Bmi-1 dependence distinguishes neural stem cell self-renewal from progenitor proliferation. *Nature* **425**: 962–967.

Molofsky AV, Slutsky SG, Joseph NM, He S, Pardal R, Krishnamurthy J *et al.* (2006). Increasing p16INK4a expression decreases forebrain progenitors and neurogenesis during ageing. *Nature* **443**: 448–452.

Munirajan AK, Ando K, Mukai A, Takahashi M, Suenaga Y, Ohira M *et al.* (2008). KIF1Bbeta functions as a haploinsufficient tumor suppressor gene mapped to chromosome 1p36.2 by inducing apoptotic cell death. *J Biol Chem* **283**: 24426–24434.

Murakami Y. (2005). Involvement of a cell adhesion molecule, TSLC1/IGSF4, in human oncogenesis. *Cancer Sci* **96**: 543–552.

Nowak K, Kerl K, Fehr D, Kramps C, Gessner C, Killmer K *et al.* (2006). BMI1 is a target gene of E2F-1 and is strongly expressed in primary neuroblastomas. *Nucleic Acids Res* **34**: 1745–1754.

Ohira M, Oba S, Nakamura Y, Isogai E, Kaneko S, Nakagawa A *et al.* (2005). Expression profiling using a tumor-specific cDNA microarray predicts the prognosis of intermediate risk neuroblastomas. *Cancer Cell* **7**: 337–350.

Orlando V, Strutt H, Paro R. (1997). Analysis of chromatin structure by *in vivo* formaldehyde cross-linking. *Methods* **11**: 205–214.

Pietersen AM, van Lohuizen M. (2008). Stem cell regulation by polycomb repressors: postponing commitment. *Curr Opin Cell Biol* **20**: 201–207.

Rajasekhar VK, Begemann M. (2007). Concise review: roles of polycomb group proteins in development and disease: a stem cell perspective. *Stem Cells* **25**: 2498–2510.

Schwartz YB, Pirrotta V. (2008). Polycomb complexes and epigenetic states. *Curr Opin Cell Biol* **20**: 266–273.

Sherr CJ. (2004). Principles of tumor suppression. *Cell* **116**: 235–246.

Sparmann A, van Lohuizen M. (2006). Polycomb silencers control cell fate, development and cancer. *Nat Rev Cancer* **6**: 846–856.

Strieder V, Lutz W. (2003). E2F proteins regulate MYCN expression in neuroblastomas. *J Biol Chem* **278**: 2983–2989.

Sugino Y, Misawa A, Inoue J, Kitagawa M, Hosoi H, Sugimoto T *et al.* (2007). Epigenetic silencing of prostaglandin E receptor 2 (PTGER2) is associated with progression of neuroblastomas. *Oncogene* **26**: 7401–7413.

Teitz T, Wei T, Valentine MB, Vanin EF, Grenet J, Valentine VA *et al.* (2000). Caspase 8 is deleted or silenced preferentially in childhood neuroblastomas with amplification of MYCN. *Nat Med* **6**: 529–535.

Valk-Lingbeek ME, Bruggeman SW, van Lohuizen M. (2004). Stem cells and cancer; the polycomb connection. *Cell* **118**: 409–418.

Viré E, Brenner C, Deplus R, Blanchon L, Fraga M, Didelot C *et al.* (2006). The Polycomb group protein EZH2 directly controls DNA methylation. *Nature* **439**: 871–874.

Westemann F, Schwab M. (2002). Genetic parameters of neuroblastomas. *Cancer Lett* **184**: 127–147.

Yan P, Mühlethaler A, Bourloud KB, Beck MN, Gross N. (2003). Hypermethylation-mediated regulation of CD44 gene expression in human neuroblastoma. *Gene Chromosomes Cancer* **36**: 129–138.

Yang Q, Zage P, Kagan D, Tian Y, Seshadri R, Salwen HR *et al.* (2004). Association of epigenetic inactivation of RASSF1A with poor outcome in human neuroblastoma. *Clin Cancer Res* **10**: 8493–8500.

Yang QW, Liu S, Tian Y, Salwen HR, Chlenski A, Weinstein J *et al.* (2003). Methylation-associated silencing of the thrombospondin-1 gene in human neuroblastoma. *Cancer Res* **63**: 6299–6310.

Yang J, Chai L, Liu F, Fink LM, Lin P, Silberstein LE *et al.* (2007). Bmi-1 is a target gene for SALL4 in hematopoietic and leukemic cells. *Proc Natl Acad Sci USA* **104**: 10494–10499.

Supplementary Information accompanies the paper on the Oncogene website (http://www.nature.com/onc)

Supplemental Figure S1

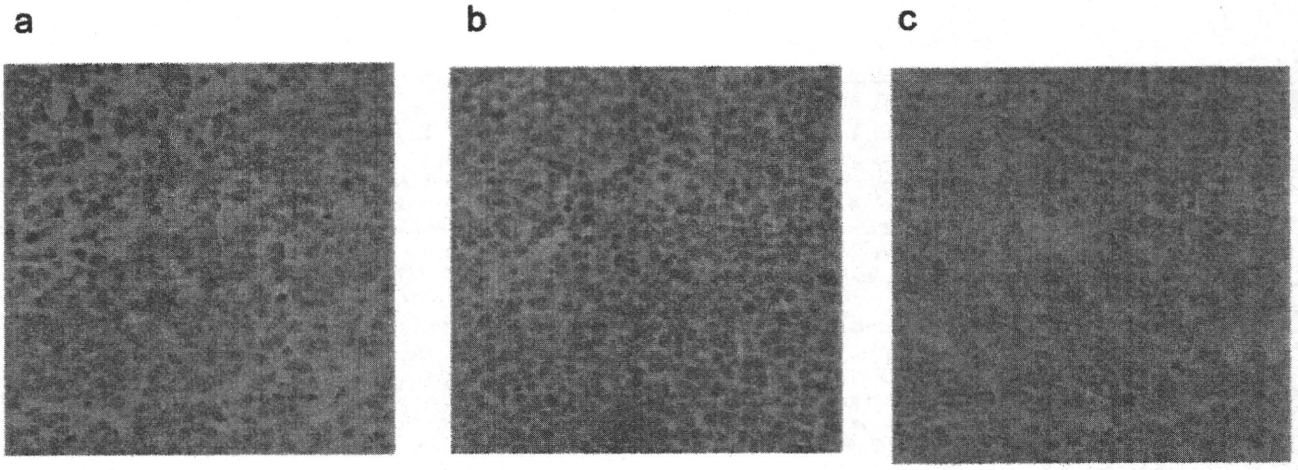

Bmi1 immunohistochemical analysis Bmi1 expression was analyzed by immunohistochemical analysis using purified rabbit polyclonal anti-Bmi1 antibody (AP2513c, ABGENT, CA, USA), as described in Materials and Methods. a. MYCN single-copy, favorable histology sample; b. MYCN amplified, unfavorable histology sample; c. MYCN amplified NB cell line-derived xenograft.

Supplemental Figure S2

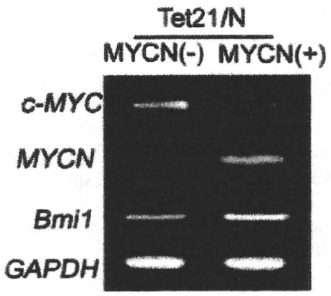

C-MYC expression in MYCN-inducible Tet21/N cells
Expressions of C-MYC, MYCN, Bmi1 and GAPDH were analyzed by semi-quantitative RT-PCR in MYCN-suppressed [(-)] and -induced [(+)] Tet21/N cells.

Supplemental Figure S3

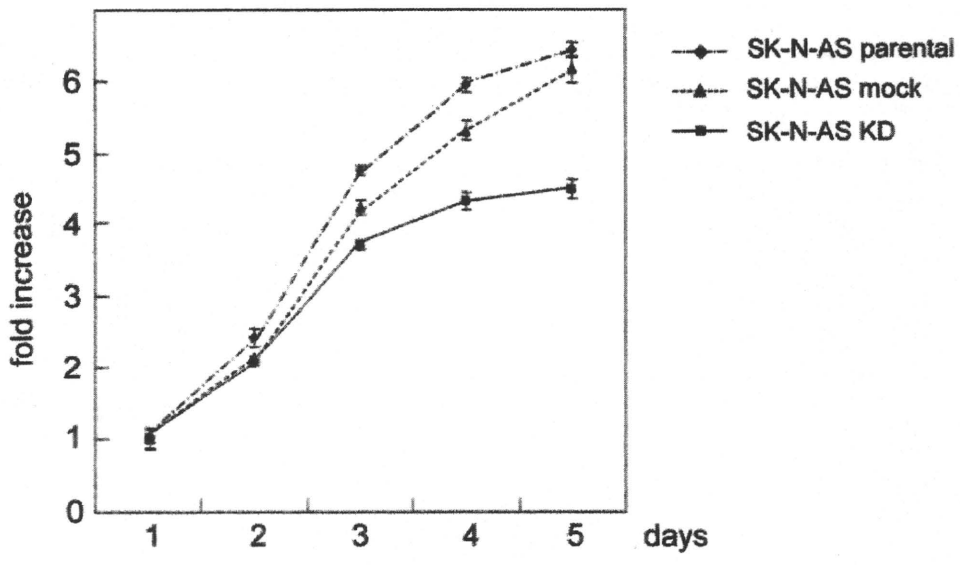

Cell proliferation assay of Bmi1-knocked down NB cells
In SK-N-AS cells, Bmi1 was knocked down by the Bmi1-shRNA expressing lentivirus, as described in Materials and Methods, and the cells were subjected to WST-8 assay. The results are averages of at least triplicate wells and standard deviation is indicated by error bars. The results are representative of three independent experiments.

Supplement Figure S4

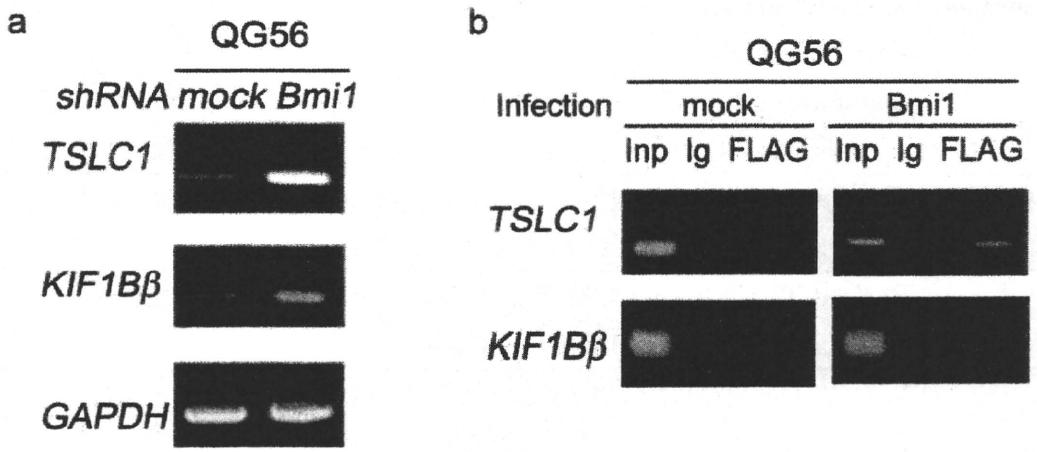

a: Bmi1-expressing virus production, and infection of Lung cancer QG56 cells were performed as described in Materials and Methods. One-week post-infection, cells were harvested, and TSLC1, KIF1Bβ and GAPDH expression was determined by RT-PCR. For KIF1Bβ expression, primers for this experiment were
F: cacccacttcttggacccta, R: ttgtagctgccactgtcctg.
b. Bmi1-shRNA-expressing virus production, and infection were performed as described in Materials and Methods. One-week post-infection, cells were harvested, and ChIP assay was performed as described.

Table S1 Primers used for semi-quantitative RT-PCR

Primer	Sequence	Accession number for cDNA
Bmi1 (RT-PCR)	F: 5'-CCAGGGCTTTTCAAAAATGA-3' R: 5'-CGTAGTGTCAGTAACGACGA-3'	NM_005180
MYCN (RT-PCR)	F: 5'-GCTTTTGCGGCCAGTATTAG-3' R: 5'-CAGGAAGAAACAGGCTAGGA-3'	NM_005378
GAPDH (RT-PCR)	F: 5'-ACCACAGTCCATGCCATCAC-3' R: 5'-TCCACCACCCTGTTGCTGTA-3'	NM_002046
GAP43 (RT-PCR)	F: 5'-GGAGAAGGCACCACTACTGC-3' R: 5'-GGCGAGTTATCAGTGGAAGC-3'	NM_001130064
Neurofillament (NF)68 (RT-PCR)	F: 5'-ACCAAGACCTCCTCAACGTG-3' R: 5'-TCAGCCTTAGACGCCTCAAT-3'	NM_006158
Vimentin (RT-PCR)	F: 5'-CCCTCACCTGTGAAGTGGAT-3' R: 5'-TCCAGCAGCTTCCTGTAGGT-3'	NM_003380
p14ARF (RT-PCR)	F: 5'-ACCCCTTCTCAGGTCCAGTT-3' R: 5'-GGCTATGGCTAGGGTTCTGA-3'	D00617
p16INK4A (RT-PCR)	F: 5'-GAATAGTTACGGTCGGAGGC-3' R: 5'-CCACCAGCGTGTCCAGGAAG-3'	NM_003380
KIF1Bβ (RT-PCR)	F: 5'-AAGGACCTTCGTGCTCA-3' R: 5'-GGAAGATGGGGATGAAGTGA-3'	AB017133
TSLC1 (RT-PCR)	F: 5'-CATTTTGGAATTTGCCTGCT-3' R: 5'-GGCAGCAGCAAAGAGTTTTC-3'	NM_014333.3

Table S2 Primers used for ChIP assay by RQ-PCR

Primer	Sequence
Bmi1 promoter (ChIP assay)	F: 5'-CTACACCGACACTAATTCCCAGG-3' R: 5'-ACGTGCTCCCCTCATTCCT-3'
TSLC1 promoter1 (ChIP assay)	F: 5'-TGGTCCCCAGCTTCCTTAG-3' R: 5'-GGAGAGGGAGTGTGGTGAAG-3'
TSLC1 promoter 2 (ChIP assay)	F: 5'-TCGGTCTGATATCAGCGATTG-3' R: 5'-GGCGGGTCTAGCTTCTTGTA-3'
TSLC1 promoter 3 (ChIP assay)	F: 5'-GCAAGGTGAGTGACGGAAAT-3' R: 5'-TGTATCAGACCGACGACTGG-3'
KIF1bβ promoter 1 (ChIP assay)	F: 5'-TTGCACGTGGAAAGTTATCTG-3' R: 5'-TCTGTGTGTGTTTCTGGATCG-3'
KIF1bβ promoter 2 (ChIP assay)	F: 5'-CACAGTGGTGTGTGCCTGTA-3' R: 5'-TGATCCTCCTGCCTCAGTCT-3'
KIF1bβ promoter 3 (ChIP assay)	F: 5'-TAAAATGTCGGGAGCCTCAG-3' R: 5'-CATTTGGATTCCTTGCTGGT-3'

Anaplastic lymphoma kinase (ALK)

中澤温子*

■歴史・背景

1994年Shiotaらはt(2;5)(p23;q35)転座をもつanaplastic large cell lymphoma (ALCL)細胞株から80 kDaのリン酸化蛋白質p80を同定した．クローニングされたcDNAの塩基配列から，N末端は既知の核蛋白質nucleophosmin*NPM*の配列と一致し，その下流の配列は血球系細胞において高発現するleukocyte tyrosine kinase (Ltk)と高い類似性をもつ新規のチロシンキナーゼ*ALK* (anaplastic lymphoma kinase)をコードすることを発見した[1]．同時期にt(2;5)の転座点をクローニングしていたMorrisらも，転座点付近に存在する遺伝子として*ALK*を報告した[2]．

■定　義

*ALK*は，インスリン受容体ファミリーに属する膜貫通型チロシンキナーゼをコードし，5 q35上の*NPM*と融合することにより，チロシンキナーゼの恒常的活性化をきたし，その下流のRAS/ERK，JAK/STAT，またはP13 K/AKT経路を活性化して細胞増殖を促進する．興味深いことに融合遺伝子のN末端の*NPM*と相同な部分を欠いたALKチロシンキナーゼの部分のみを発現させた細胞にはコロニー形成能が認められず，*NPM-ALK*の細胞癌化能には*NPM*のプロモーター部分が必須である[3]．ALKは，*NPM*以外にもさまざまな遺伝子との間に転座による融合遺伝子を形成することが知られている(**表1**)[4]．また，神経芽腫では6.1%に*ALK*のミスセンス変異が検出され，家族性神経芽腫の家系では*ALK*のgerm line変異が認められる．変異*ALK*は，NIH3 T3細胞に遺伝子導入することにより野生型に比べて強いコロニー形成能を示し，ヌードマウスに腫瘍を形成する[5]．ALCLやこれらの腫瘍では，転座や変異によってALKの自己リン酸化が起こり活性が上昇している．最近，非小細胞肺癌でも*EML4-ALK*融合遺伝子が同定され[6]，ALK阻害剤が分子標的療法として注目されている．

■ALK陽性未分化大細胞型リンパ腫 (ALK$^+$ALCL)

ALK$^+$ALCLは，30歳以下の若年者に多く，ALK陰性ALCLに比較して予後良好である[7]．豊富な細胞質と多形性に富んだ特異な形態の核を有する大型細胞(hallmark cell)のびまん性増殖からなり，腫瘍細胞はALK，CD30陽性である(common pattern)．リンパ節の辺縁洞への浸潤や血管周囲に腫瘍細胞が配列するperivascular patternがしばしば認められる．組織学的亜型として，組織球の増生が目立つlymphohistiocytic pattern (LH；10%)，不整な核を有する小型から中型の腫瘍細胞が増殖するsmall cell pattern (SC；5～10%)，結節硬化型ホジキンリンパ腫に類似したHodgkin-like pattern (3%)が認められ，これらの亜型が混在する場合にはmixed patternとして各亜型を併記する．いずれの亜型にも割合はさまざまであるがhallmark cellが認められる[7]．小児例355例の解析では，perivascular patternまたはLH・SC成分を有する症例は皮膚，縦隔，臓器浸潤の頻度が高く，また有意に再発率が高い[8]．ALKの発現は正常組織においては脳および末梢神経の一部の細胞に限局しており血液細胞での発現は認められないため，抗ALK染色は鑑別診断に有用である．また転座相手により染色パターンが異なり，t(2;5)では核と細胞質が陽性となる(**図1，2**)．small cell patternで認められる小型の腫瘍細胞では，CD30は弱陽性か陰性で，ALKは核のみに陽性となる[7]．ALKの染色パターンによる臨床像や予後の差はない[7,8]．

■ALK陰性未分化大細胞型リンパ腫 (ALK$^-$ALCL)

WHO分類第4版では，ALK陽性ALCLと組織学的には区別できないがALK陰性であるT細胞性リンパ腫がALK陰性ALCL (ALK$^-$ALCL)として独立して

*国立成育医療研究センター病理診断科

0287-3745/10/¥100/頁/JCOPY

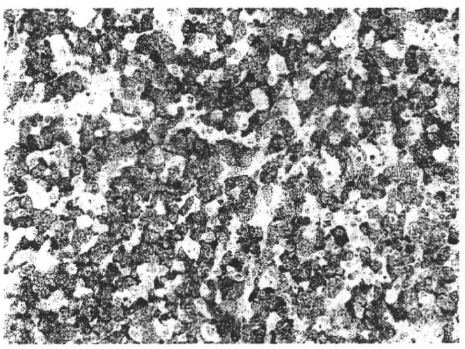

図1

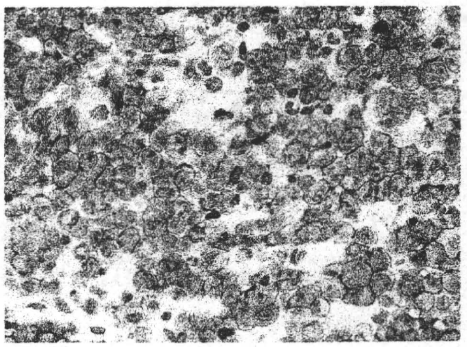

図2

図1　anaplastic large cell lymphoma, ALK-positive (common pattern)　抗ALK染色では核と細胞質がびまん性に陽性となる．PCRにより*NPM-ALK*融合遺伝子が検出された．

図2　anaplastic large cell lymphoma, ALK-positive (common pattern)　抗ALK染色では細胞質がびまん性に陽性となり，細胞膜が強く染色される．PCRにより*TPM3-ALK*融合遺伝子が検出された．

表1　ALK$^+$ALCLにおける*ALK*転座と融合遺伝子[6,8]

Chromosomal abnormality	Fusion protein	ALK staining pattern	頻度	同じFusion proteinを示す疾患
t(2;5)(p23;q35)	NPM-ALK	Nuclear,diffuse cytoplasmic	84%	DLBCL
t(1;2)(q25;p23)	TPM3-ALK	Diffuse cytoplasmic with peripheral intensification	13%	IMT
inv(2)(p23;q35)	ATIC-ALK	Diffuse cytoplasmic	1%	
t(2;3)(p23;q21)	TFG-ALK	Diffuse cytoplasmic	<1%	
t(2;17)(p23;q23)	CTLC-ALK	Granular cytoplasmic	<1%	DLBCL
t(2;X)(p23;q11-12)	MSN-ALK	Membrane staining	<1%	
t(2;19)(p23;q13.1)	TPM4-ALK	Diffuse cytoplasmic	<1%	SCC
t(2;22)(p23;q11.2)	MYH9-ALK	Diffuse cytoplasmic	<1%	
t(2;17)(p23;q25)	ALO17-ALK	Diffuse cytoplasmic	<1%	

DLBCL：diffuse large B-cell lymphoma，IMT：inflammatory myofibroblastic tumor，SCC：squamous cell carcinoma of esophagus.

組み入れられた[7]．ALK$^-$ALCLは，さまざまなCD30陽性リンパ腫(peripheral T-cell lymphoma, NOS, CD30$^+$enteropathy-associated T-cell lymphoma, Hodgkin lymphoma)との鑑別が必ずしも容易ではなく，また臨床病理学的に十分に確立された診断名とはいえない．皮膚原発ALCLはALK陰性で，ALK$^-$ALCLと同様の組織所見，免疫組織化学染色所見を示すため，鑑別診断には詳細な臨床情報が必要となる．

■ ALK陽性大細胞型B細胞リンパ腫(ALK$^+$DLBCL)

ALK$^+$DLBCLは男性に多く(男性：女性=5：1)，予後不良である．腫瘍細胞は，plasmablasticな形態を呈しEMA，CD138，cytoplasmic Ig陽性であるが，CD20，CD79a，CD3，CD30は陰性である．t(2;17)が多くみられるが，t(2;5)を示す例もある[4]．

文　献

1) Shiota, M., Fujimoto, J., Semba, T. et al.：Hyperphosphorylation of a novel 80 kDa protein-tyrosine kinase similar to Ltk in a human Ki-1 lymphoma cell line, AMS3. Oncogene 1994, **9**：1567-1574
2) Morris, S.W., Kirstein, M.N., Valentine, M.B. et al.：Fusion of a kinase gene, ALK, to nucleolar protein gene, NPM, in non-Hodgkin's lymphoma. Science 1994, **263**：1281-1284
3) Fujimoto, J., Shiota, M., Iwahara, T. et al.：Characterization of the transforming activity of p80, a hyperphosphorylated protein in a Ki-1 lymphoma cell line with chromosomal translocation t(2;5). Proc Natl Acad Sci USA 1996, **93**：4181-4186
4) Palmer, R.H., Vernersson, E., Grabbe, C. et al.：Anaplastic lymphoma kinase：signalling in development and disease. Biochem J 2009, **420**：345-361
5) Chen, Y., Takita, J., Choi, Y.L. et al.：Oncogenic mutations of ALK kinase in neuroblastoma. Nature 2008, **455**：971-974
6) Soda, M., Choi, Y.L., Enomoto, M. et al.：Identification of the transforming EML4-ALK fusion gene in non-small-cell lung cancer. Nature 2007, **448**：561-566
7) Swerdlow, S.H., Campo, E., Harris, N.L. et al.：WHO Classification of Tumours of Hematopoietic and Lymphoid Tissues, 4th ed., IARC Press, Lyon, 2008, 312-319
8) Lamant, L., McCarthy, K., d'Amore, E.S.G. et al.：Prognostic impact of morphologic and phenotypic features of childhood ALK-positive anaplastic large cell lymphoma (ALCL)：Results of the ALCL99 study. Hematology Meeting Reports 2009, **3**：42

Pediatr Surg Int (2011) 27:231–236
DOI 10.1007/s00383-010-2781-4

ORIGINAL ARTICLE

The genetic and clinical significance of MYCN gain as detected by FISH in neuroblastoma

Ryota Souzaki · Tatsuro Tajiri · Risa Teshiba · Mayumi Higashi · Yoshiaki Kinoshita · Sakura Tanaka · Tomoaki Taguchi

Published online: 3 November 2010

Abstract
Purpose *MYCN* amplification (*MYCN*-A) is a strong prognostic factor in neuroblastoma (NB). *MYCN* gain which is a low level of *MYCN*-A as determined by FISH. It is unclear whether the *MYCN* gain is the pre-status of *MYCN*-A. This study assessed the status of *MYCN* gene and chromosome 2p of *MYCN*-A, *MYCN* gain and no *MYCN* amplification using a single nucleotide polymorphism (SNP) array, and the clinical implication of *MYCN* gain in NB.
Methods The status of the *MYCN* gene was determined by FISH in 47 primary NB samples and the status of chromosome 2p in all cases was analyzed using an SNP array.
Results 8 of the 47 cases analyzed using FISH showed *MYCN*-A, 7 cases showed *MYCN* gain and 32 cases showed no *MYCN* amplification. An SNP array analysis showed that only 2 of 8 cases with *MYCN*-A by FISH had both amplification of *MYCN* region and distal 2p gain and other 6 cases had amplification of the *MYCN* region without distal 2p gain. All 7 cases with *MYCN* gain by FISH had distal 2p gain without amplification of the *MYCN* region, and all 32 cases with no *MYCN* amplification by FISH demonstrated neither the amplification of the *MYCN* region nor the 2p gain. 5-year overall survival rate of patients with *MYCN* gain ($n = 7$, 71.4%) was not significant different from that of patients with no *MYCN* amplification ($n = 32$, 90.6%) by FISH ($p = 0.11$).
Conclusions These results suggested that the *MYCN* gain detected by FISH represents the 2p gain, and the *MYCN* gain is not considered to represent the pre-status of *MYCN* amplification.

Keywords Neuroblastoma · MYCN gain · 2p gain

R. Souzaki (✉) · T. Tajiri · R. Teshiba · M. Higashi · Y. Kinoshita · S. Tanaka · T. Taguchi
Department of Pediatric Surgery, Graduate School of Medical Sciences, Kyushu University, 3-1-1 Maidashi, Higashi-ku, Fukuoka 812-8582, Japan
e-mail: ryotas@pedsurg.med.kyushu-u.ac.jp

Introduction

Neuroblastoma (NB) is the most common solid malignant tumor in children. It arises from the sympathetic nervous system and usually occurs in the adrenal medulla. *MYCN* gene amplification occurs in approximately 25% of primary NB, and this is an unfavorable prognostic factor in NB [1–3].

It is important to accurately estimate the status of *MYCN* gene amplification for the treatment of NB. The recommended assay for the amplification of the *MYCN* gene in an NB sample is quantitative polymerase chain reaction (Q-PCR) and fluorescence in situ hybridization methods (FISH) rather than Southern blotting (SB) [4–6]. A previously study reported that an FISH analysis shows that 6% of NB samples have cells *MYCN* gain [7] which indicates that the additional *MYCN* gene signals increase equal to or less than fourfold in relation to the chromosome 2 signals [8]. It is unclear whether the *MYCN* gain represents the pre-status of *MYCN* amplification. Furthermore, the clinical significance of *MYCN* gain is unclear.

On the other hand, NB without *MYCN* gene amplification has a variety of clinical courses because it has significant genetic instability at the chromosomal level as allelic loss and gain or rearrangement, such as a 1p loss, 3p loss, 11q loss and 17q gain [9, 10]. A distal unbalanced 2p gain is also seen in primary NBs [11–13] and is

associated with unbalanced translocation or distal 2p duplication [14, 15]. This distal 2p gain region usually includes a *MYCN* gene region which is located at 2p24, but the prognosis associated with a low level of the *MYCN* gene increase with a 2p distal gain remains to be elucidated.

This study analyzed the status of the *MYCN* gene using FISH and the status of chromosome 2p using single nucleotide polymorphism (SNP) array to assess the genetic status of *MYCN* gain.

Materials and methods

Clinical data of patients and biologic data of neuroblastoma samples

Patients with NB, evaluated at the Department of Pediatric Surgery Kyushu University, Fukuoka, Japan, were diagnosed between April 1988 and March 2008. The tumor was staged according to the International Neuroblastoma Staging System (INSS). All of the parents of the patients provided their informed consent for tumor preservation and the biological analysis before surgery. This study was performed according to ethics guidelines for the clinical studies by Ministry of Health, Labour and Welfare. Forty-seven NB samples were obtained from untreated patients with neuroblastoma. The patients included 24 males and 23 females, and 12 were stage 1 as INSS, 4 were stage 2, 7 were stage 3, 20 were stage 4, and 4 were stage 4S. Twenty-five had been diagnosed when they were younger than 12 months of age (median 12 months, 0–96 months). Eight patients were identified by a mass screening system in Japan at 6 months. The *MYCN* gene amplification was quantified using FISH, Q-PCR and SB [16] in all 47 cases. An SNP array analysis was performed on a total of all 47 samples. DNA ploidy was determined by flow cytometry in 46 specimens [17].

FISH method

The gene dosage of the *MYCN* gene was determined by an FISH analysis as described previously [18]. The *MYCN* gene probe (LSI N-MYC SO, Vysis) or *MYCN* gene and the alpha satellite region of human chromosome 2 probes (LSI N-MYC SG/CEP 2 SO DNA probe, Vysis) were used. The signals representing the *MYCN* gene and the centromeric region of chromosome 2 were counted in 100 cells on each slide. The *MYCN* amplification was defined as an increase in over fourfold of *MYCN* signals in relation to the number of chromosome 2 signals in a dual color probe, or over 8 *MYCN* signals in single color probe. Additional copies equal to or less than fourfold in the dual color probe were defined as *MYCN* gain cells. In addition, no *MYCN* amplification was defined that *MYCN* signals equal to chromosome 2 signals such as disomy and trisomy.

SNP array

DNA was extracted from tumor samples and purified using the standard method. The DNA was subjected to SNP array analysis using Human CMV370-Duo (Illumina, San Diego, CA) according to the manufacturer's protocol. Genomic profiles were created using the Illumina Genome Viewer (IGV) and Chromosome Browser (ICV) of Illumina's BeadStudio3.0 software.

Quantitative PCR (TaqMan)

The gene dosage of the *MYCN* gene was determined by a Q-PCR analysis as described previously [4, 18, 19]. The *N*-acetylglucosamine kinase gene (*NAGK*) was used as an internal control gene to determine the *MYCN* gene dosage [18, 19]. The primers and the TaqMan probe for *MYCN* gene were MYCN forward, 5′-GTGCTCTCAATTCT CGCCT-3′; *MYCN* reverse, 5′-GATGGCCTAGAGGAGG GCT-3′; *MYCN* Probe, 5′-FAM-CACTAAAGTTCCTTCC ACCCTCTCCT-TAMRA-3′. The primers and TaqMan probe for *NAGK* gene were *NAGK* forward, 5′-TGGG CAGACACATCGTAGCA-3′; *NAGK* reverse, 5′-CACCT TCACTCCCACCTCAAC-3′; and *NAGK* probe, 5′-VIC-TGTTGCCCGAGATTGACCCGGT-TAMRA-3′. Q-PCR was performed in a final volume of 30 lL, and each sample was evaluated in duplicate. Each reaction mixture contained 0.1 pmol/lL TaqMan probe, 0.2 pmol/lL each primer, 1× TaqMan PCR master mix and extracted DNA. PCR amplification was started with 2 min incubation at 50°C, followed by a denaturation step of 10 min at 95°C, and then 40 cycles at 95°C for 15 s and 60°C for 1 min. The genes quantified using the ABI Prism 7700 Sequence Detection System (Applied Biosystems). Genomic DNA from normal lymphocyte cells from healthy donors was serially diluted to establish the calibration curve.

Statistics

The survival curve was estimated using the Kaplan–Meier procedure and then it was statistically evaluated by the log-rank test. The χ^2 test and Fisher's exact test was used to compare the incidence of typical unbalanced gain and loss of NB in the patients with *MYCN* gain and no *MYCN* amplification. The results were considered to be significantly different when $p < 0.05$.